Simultaneous analyses of photoinduced electron transfer in the wild type and four single substitution isomers of the FMN binding protein from Desulfovibrio vulgaris, Miyazaki F

ARTICLE *in* PHYSICAL CHEMISTRY CHEMICAL PHYSICS · FEBRUARY 2011

Impact Factor: 4.49 · DOI: 10.1039/c0cp02634d · Source: PubMed

4 AUTHORS, INCLUDING:

Fumio Tanaka
Chulalongkorn University
112 PUBLICATIONS **1,134** CITATIONS

SEE PROFILE

PCCP

Dynamic Article Links

Cite this: *Phys. Chem. Chem. Phys.*, 2011, **13**, 6085–6097

www.rsc.org/pccp

PAPER

Simultaneous analyses of photoinduced electron transfer in the wild type and four single substitution isomers of the FMN binding protein from *Desulfovibrio vulgaris*, Miyazaki F†

Nadtanet Nunthaboot,[a] Somsak Pianwanit,*[b] Sirirat Kokpol[b] and Fumio Tanaka*[c]

Received 23rd November 2010, Accepted 17th January 2011
DOI: 10.1039/c0cp02634d

The mechanism of photoinduced electron transfer (PET) from the aromatic amino acids (Trp32, Tyr35 and Trp106) to the excited flavin mononucleotide (FMN) in the wild type (WT) and four single amino acid substitution isomers (E13T, E13Q, W32A and W32Y) of FMN binding protein (FBP) from the *Desulfovibrio vulgaris* (Miyazaki F) were simultaneously analyzed (Method A) with the Marcus–Hush (MH) theory and Kakitani–Mataga (KM) theory using ultrafast fluorescence dynamics of these proteins. In addition, the PET mechanism of the WT, E13T and E13Q FBP systems (Method B) were also analyzed with both MH and KM theories. The KM theory could describe all of the experimental fluorescence decays better than the MH theory by both Methods A and B. The PET rates were found to largely depend on the electrostatic energies between photo-products, isoalloxazine (Iso) anion and the PET donor cations, and the other ionic groups, and hence on static dielectric constants. The dielectric constant (ε_0^{DA}) around the PET donors and acceptor was separately determined from those (ε_0^j, j = WT, E13T, E13Q, W32Y and W32A) in the domain between the Iso anion or the donor cations and the other ionic groups in the proteins. The values of ε_0^{DA} were always lower than those of ε_0^j, which is reasonable because no amino acid exists between the PET donors and acceptor in all systems. The values of the dielectric constants ε_0^j (j = WT, E13T and E13Q) were similar to those obtained previously from the analysis of the crystal structures and the average lifetimes of these FBP proteins. Energy gap law in the FBP systems was examined. An excellent parabolic function of the logarithms of the PET rates was obtained against the total free energy gap. The PET in these FBP isomers mostly took place in the so-called normal region, and partly in the inverted region.

I. Introduction

Electron transfer phenomena have been important subjects in the fields of physics, chemistry and biology.[1,2] The photo-induced electron transfer (PET) plays an essential role in photosynthetic systems.[3] In the last decade a number of new flavin photoreceptors have been found,[4] including the BLUF (blue-light using flavin) units of the flavin photoreceptors that contain Tyr and/or Trp near isoalloxazine (Iso). The PET from Tyr to the excited Iso (Iso*) is considered to be the first step of the photo-regulation for photosynthesis in AppA[5] and pili-dependent cell motility in TePixD[6] and Slr1694[6] in the BLUF-containing photoactive bacteria.

Fluorescence quenching of flavins by various substances, including aromatic amino acids, was first investigated by Weber.[7] McCormick demonstrated a remarkable quenching of fluorescence from Iso* by Trp in series of compounds in which Iso and Trp are covalently linked.[8] Time-resolved fluorescence of flavins and flavoproteins has been reviewed by van den Berg and Visser.[9] Most of the flavoproteins, other than the flavin photoreceptors, contain the aromatic amino acids Trp and Tyr near the Iso and these flavoproteins are practically non-fluorescent. However, they emit fluorescence with very short lifetimes following excitation with a sub-picosecond light pulse.[10–15] This remarkable fluorescence quenching is considered to be ascribed to the ultrafast PET in these flavoproteins from the Trp and/or Tyr to the Iso*.[16–19]

Since the seminal works on electron transfer theory by Marcus,[20] several researchers have further developed the PET theory.[21,22] However, these have been modeled for PET

[a] *Department of Chemistry, Faculty of Science, Mahasarakham University, Mahasarakham, 44150, Thailand*
[b] *Department of Chemistry, Faculty of Science, Chulalongkorn University, Bangkok, 10330, Thailand. E-mail: somsak.t@chula.ac.th*
[c] *Department of Biochemistry, Center for Excellence in Protein Structure and Function, Faculty of Science, Mahidol University, Bangkok, 10400, Thailand. E-mail: fukoh2003@yahoo.com*
† Electronic supplementary information (ESI) available. See DOI: 10.1039/c0cp02634d

in bulk solution and it is not clear whether these theories are applicable to PET in proteins. To this end it is required to establish a method to quantitatively analyze PET in proteins. The PET rates in flavoproteins have been analyzed with ultrafast fluorescence dynamics and Kakitani and Mataga (KM) theory using the atomic coordinates obtained by molecular dynamics simulation (MD).[23–26]The procedure to determine the unknown PET parameters was performed as follows: (1) the time-dependent atomic coordinates of flavoproteins were obtained by MD, (2) the PET rates were calculated using a PET theory and the atomic coordinates with a set of trial PET parameters, (3) the parameters were varied until the best-fit between the calculated and observed fluorescence decays was obtained, according to a non-linear least squares method.

Recently, it has been demonstrated that disappearance of only one negative charge in the wild type (WT) flavin mononucleotide (FMN) binding proteins (FBP) modifies the ultrafast fluorescence dynamics, and consequentially the PET rates in E13T and E13Q.[27] This suggests that electrostatic interactions between ionic photoproducts and the other ionic groups in the proteins are the most influential factors upon the PET rate from Trp and/or Tyr to Iso*, together with the donor–acceptor distances. Static (averaged) lifetimes of the WT FBP, and the single substitution E13T and E13Q isomers, have been analyzed from their X-ray structures. It is important to obtain common PET parameters in FBP protein systems, because some of them can be used for electron transfer processes in FBP without light. In the present work, we have simultaneously analyzed the ultrafast fluorescence dynamics of the WT and four single substitution isoforms (E13T, E13Q, W32Y and W32A) of FBPs with Marcus and Hush (MH) theory[20] and KM theory,[22] to determine the common PET parameters, and also to establish the method of the PET analysis. The effect of the disappearance of the negative charge in the WT FBP at Glu13 on the PET rate was also examined with ultrafast fluorescence dynamics of these systems and the protein structures obtained by MD.

II. Methods of analyses

MD calculation

The starting structures of the WT and its mutated FBPs were obtained by using the X-ray structure of the *D. vulgaris* (Miyazaki F) WT FBP (PDB code 1FLM).[28] In the E13T and E13Q single substitution isomers, the glutamate at position 13 was replaced by threonine and glutamine, respectively, and the replacement of amino acids from the WT was conducted using the LEap module implemented in AMBER 8.[29] All calculations were carried out using the AMBER 8 suite of programs. The parm99 force field[30] was used to describe the protein atoms whereas force field parameters for Iso were obtained from Schneider and Suhnel.[31] All missing hydrogen atoms of the protein were added using the LEap module of AMBER 8. The simulated systems were subsequently solvated with a cubic box of 6336 TIP3P water molecules. This is almost comparable to that of 6345 and 6347 in the case of W32Y and W32A, respectively.[24]

The electroneutrality of the systems was attained by adding 1 chloride counterion. The added water molecules were first minimized, while the protein and Iso coordinates were kept fixed. The entire system was then optimized using 2000 steps of steepest descent and conjugated gradient minimizations. Afterwards, the whole system was heated from 10 K to 298 K over 50 ps and was further equilibrated under periodic boundary conditions at 298 K. The systems were set up under the isobaric–isothermal ensemble (NPT) with a constant pressure of 1 atm and constant temperature of 298 K. Electrostatic interaction was corrected by the Particle Mesh Ewald method.[32] The SHAKE algorithm[33] was employed to constrain all bonds involving hydrogen atoms. A cutoff distance of 1 nm was employed for non-bonded pair interactions. MD based calculations were performed with the time steps of 2 fs and the coordinates of the MD snapshots were collected every 0.01 ps. The simulations were performed over 5 ns. Data collected during the last 3 ns were used to analyze and to compare with that from previous MDs of W32Y and W32A FBP systems.[24]

PET theory

MH,[20] Bixon and Jortner (BJ),[21] and KM theories[22] were applied for the PET process in the WT FBP.[23] The observed fluorescence decay was satisfactorily reproduced with MH and KM theories. However, only the decay of the WT FBP was examined by these PET theories. In the present work, we have simultaneously examined five decays of WT, E13T, E13Q, W32Y and W32A FBP systems with both MH and KM theories.

The PET rate from a donor k to Iso* in the jth FBP system given by MH theory (k_{MH}^{jk}) is expressed as eqn (1).[20]

$$k_{\mathrm{MH}}^{jk} = \frac{2\pi}{\hbar}\frac{H_q^2}{\sqrt{4\pi\lambda_{\mathrm{S}}^{jk}k_{\mathrm{B}}T}} \times \exp\left[-\frac{\left\{\Delta G_q^0 - e^2/\varepsilon_0^{DA}R_{jk} + \lambda_{\mathrm{S}}^{jk} + ES_j(k)\right\}^2}{4\lambda_{\mathrm{S}}^{jk}k_{\mathrm{B}}T}\right] \quad (1)$$

where H_{q} is the electronic interaction energy between Iso* and the donor q (Trp or Tyr), assuming that H_{q} depends only on q, and not on j and k. R_{jk} is the center-to-center distance between Iso and the PET donor k in the jth FBP system. For this FBP, j = 1, 2, 3, 4, and 5 for the WT, E13T, E13Q, W32Y and W32A isoforms, respectively, whilst k = 0 for Iso, k = 1 for Trp32 (Tyr32 in W32Y), k = 2 for Tyr35 and k = 3 for Trp106. The PET rate may be dependent on both j and k. $\hbar$, k_{B}, T and e are the reduced Planck's constant, Boltzmann's constant, temperature (298 K) and electron charge, respectively. $\varepsilon_0^{\mathrm{DA}}$ is a static dielectric constant of medium between PET donors and acceptor. $ES_j(k)$ is a net electrostatic (ES) energy between the kth aromatic ionic species and all the other ionic groups in the jth FBP system, as described below. $\lambda_{\mathrm{S}}^{jk}$ is the solvent reorganization energy of the Iso* and the kth donor in the jth FBP system, as shown by eqn (2).

$$\lambda_{\mathrm{S}}^{jk} = e^2\left(\frac{1}{2a_{\mathrm{Iso}}} + \frac{1}{2a_q} - \frac{1}{R_{jk}}\right)\left(\frac{1}{\varepsilon_\infty} - \frac{1}{\varepsilon_0^{\mathrm{DA}}}\right) \quad (2)$$

Here, a_{Iso} and a_q are the radii of Iso and the donor q (Trp or Tyr), assuming these reactants are spherical, and ε_∞ is optical dielectric constant (a value of 2 being used). The radii of Iso, Trp and Tyr were determined as previously reported,[23–26] with values of a_{Iso} = 0.224 nm, and a_{Trp} = 0.196 nm and a_{Tyr} = 0.173 nm being used.

The standard free energy gap (ΔG_q^0) was expressed with the ionization potential (E_{IP}^q) of the PET donor q (Trp or Tyr), as eqn (3).

$$\Delta G_q^0 = E_{IP}^q - G_{Iso}^0 \quad (3)$$

where G_{Iso}^0 is the standard Gibbs energy related to the electron affinity of Iso*. The values of E_{IP}^q for Trp and Tyr were 7.2 eV and 8.0 eV, respectively.[34]

The PET rate from the donor k to Iso* in the jth FBP system, as given by the KM theory (k_{KM}^{jk}), is expressed as eqn (4).[22]

$$k_{KM}^{jk} = \frac{\nu_0^q}{1+\exp\{\beta^q(R_{jk}-R_0^q)\}}\sqrt{\frac{k_B T}{4\pi\lambda_S^{jk}}} \times \exp\left[-\frac{\left\{\Delta G_q^0 - e^2/\varepsilon_0^{DA}R_{jk} + \lambda_S^{jk} + ES_j(k)\right\}^2}{4\lambda_S^{jk}k_B T}\right] \quad (4)$$

Here ν_0^q is an adiabatic frequency, β^q is the PET process coefficient, and R_0^q is a critical distance between the adiabatic and non-adiabatic PET processes. These quantities depend only on q (Trp or Tyr), and when $R_{jk} < R_0^q$ the PET process may be adiabatic, whereas when $R_{jk} > R_0^q$ the PET process is non-adiabatic. The meanings of all the other quantities are the same as those in MH theory.

ES energy in the proteins

Proteins, including the FBPs, contain many ionic groups, which may influence the PET rate. The WT, and the single-substitution E13T and E13Q isoforms of the *D. vulgaris* (Miyazaki F) FBP contain Trp32, Tyr35 and Trp106 as potential PET donors, whilst W32Y contains Tyr32, Tyr35 and Trp106 as PET donors and W32A contains only Tyr35 and Trp106. The cofactor in all these FBP systems is FMN, which has two negative charges at the phosphate. The WT, W32Y and W32A isoforms contain 8 Glu, 5 Asp, 4 Lys and 9 Arg residues, whereas E13T and E13Q have 7 Glu residues since the Glu13 was replaced by the neutral Thr13 and Gln13, respectively. The ES energy between the Iso anion or donor k cation, and all the other ionic groups in the FBP system j is expressed by eqn (5):

$$E_j(k) = \sum_{i=1}^{n}\frac{C_k C_{Glu}}{\varepsilon_0^j R_k(Glu-i)} + \sum_{i=1}^{5}\frac{C_k C_{Asp}}{\varepsilon_0^j R_k(Asp-i)} + \sum_{i=1}^{4}\frac{C_j C_{Lys}}{\varepsilon_0^j R_k(Lys-i)} + \sum_{i=1}^{9}\frac{C_j C_{Arg}}{\varepsilon_0^j R_k(Arg-i)} + \sum_{i=1}^{2}\frac{C_j C_P}{\varepsilon_0^j R_k(P-i)} \quad (5)$$

where n = 8 for the WT, W32Y and W32A, and n = 7 for the E13T and E13Q isoforms. Here, k = 0 for the Iso anion, k = 1 for $Trp32^+$ ($Tyr32^+$ in W32Y), k = 2 for $Tyr35^+$ and k = 3 for $Trp106^+$. ε_0^j is the static dielectric constant of the jth FBP system. C_k is the charge of the aromatic ionic species k, and is $-e$ for k = 0 (Iso anion), $+e$ for k = 1 to 3. $C_{Glu}(=-e)$, $C_{Asp}(=-e)$, $C_{Lys}(=+e)$, $C_{Arg}(=+e)$ and $C_P(=-e)$ are the charges of Glu, Asp, Lys, Arg and phosphate anions, respectively. We assumed that these groups are all in an ionic state in solution. Distances between the aromatic ionic species k and the ith Glu (i = 1 – 8 or 7) are denoted as $R_k(Glu - i)$, those between k and the ith Asp (i = 1 – 4) are denoted as $R_k(Asp - i)$, and so on.

$ES_j(k)$ in eqn (1) was expressed as follows:

$$ES_j(k) = E_j(0) + E_j(k) \quad (6)$$

Here, j varies from 1 to 5 in Method A and 1 to 3 in Method B with k values from 1 to 3 (kth PET donor), as given in eqn (5).

Fluorescence decays. The experimental fluorescence decay functions of the WT, W32Y and W32A FBP isoforms have been reported by Chosrowjan *et al.*,[14,15] as given by eqn (7)–(9), respectively, whereas those for E13T and E13Q are given by eqn (10) and (11)[27] respectively.

$$F_{obs}^{WT} = 0.96\exp(-t/0.167) + 0.04\exp(-t/1.5) \quad (7)$$

$$F_{obs}^{W32Y} = 0.23\exp(-t/3.4) + 0.74\exp(-t/18.2) + 0.03\exp(-t/96) \quad (8)$$

$$F_{obs}^{W32A} = \exp(-t/30.1) \quad (9)$$

$$F_{obs}^{E13T} = 0.86\exp(-t/0.107) + 0.12\exp(-t/1.5) + 0.02\exp(-t/30) \quad (10)$$

$$F_{obs}^{E13Q} = 0.85\exp(-t/0.134) + 0.12\exp(-t/0.746) + 0.03\exp(-t/30) \quad (11)$$

The lifetimes are indicated in units of ps. The calculated decay function of the jth FBP system with MH theory is expressed by eqn (12).

$$F_{calc}^{j}(t) = \left\langle \exp\left[-\left\{\sum_{k=1}^{3} k_{MH}^{k}(t')\right\}t\right]\right\rangle_{AV} \quad (12)$$

The calculated decay function of the jth FBP system with KM theory is expressed by eqn (13):

$$F_{calc}^{j}(t) = \left\langle \exp\left[-\left\{\sum_{k=1}^{3} k_{KM}^{k}(t')\right\}t\right]\right\rangle_{AV} \quad (13)$$

The fluorescence decays of the WT, E13T and E13Q FBP isoforms were calculated up to 3 ps with 0.003 ps time intervals, whilst that for the W32Y and W32A isoforms were calculated up to 20 ps with 0.02 ps intervals. Note that $\langle\ldots\rangle_{AV}$ denotes the averaging procedure of the exponential function in eqn (12) and (13), and was performed over t' up to 2 ns with 0.1 ps time intervals for the WT, W32Y and W32A isoforms, and up to 3 ns with 0.1 ps intervals for the E13T and E13Q isoforms. In eqn (12) and (13) we assumed that the decay functions at every instant of time (t') during the MD time range can always be expressed by an exponential function. The present method is equivalent to the reported one[35] when the

time range ($t' = 2$–3 ns) of MD data is much longer than that for the fluorescence data (t at most 20 ps). The mathematical basis of the present method is described in ESI† A.

In the MH based analysis, the unknown PET parameters were H_{Trp}, H_{Tyr}, G^0_{Iso}, ε_0^{WT}, ε_0^{E13T}, ε_0^{E13Q} and ε_0^{DA}in Methods A and B, plus ε_0^{W32Y} and ε_0^{W32A} in Method A. In the KM based analysis the unknown parameters were G^0_{Iso}, ε_0^{WT}, ε_0^{E13T}, ε_0^{E13Q} and ε_0^{DA}in Methods A and B, plus ε_0^{W32Y} and ε_0^{W32A} in Method A. The previously reported values for ν_0^q, β^q and R_0^q (q = Trp or Tyr) were used.[27] To compare the results obtained with crystal structures[27] we also analyzed ET parameters by Method B. The chi-squared value of the jth FBP system between the observed and calculated fluorescence intensities (χ_j^2) is defined by eqn (14).

$$\chi_j^2 = \frac{1}{N}\sum_{i=1}^{N}\frac{\{F^j_{calc}(t_i) - F^j_{obs}(t_i)\}^2}{F^j_{calc}(t_i)} \qquad (14)$$

Here, N denotes the number of time intervals of the fluorescence decay, and was 1000 for all evaluations. The deviation between the observed and calculated intensities is expressed by eqn (15).

$$Dev_j(t_i) = \frac{\{F^j_{calc}(t_i) - F^j_{obs}(t_i)\}}{\sqrt{F^j_{calc}(t_i)}} \qquad (15)$$

We determined all of the PET parameters in the MH and KM theories by the two methods:

$$\text{Method A: } \chi_5^2 = \chi^2_{WT} + \chi^2_{E13T} + \chi^2_{E13Q} + \chi^2_{W32Y} + \chi^2_{W32A} \qquad (16)$$

$$\text{Method B: } \chi_3^2 = \chi^2_{WT} + \chi^2_{E13T} + \chi_{E13Q}{}^2 \qquad (17)$$

The PET parameters were determined both by MH and KM theories so as to obtain the minimum values of χ_5^2 in Method A and χ_3^2 in Method B, by means of a non-linear least squares method, according to the Marquardt algorithm, as previously reported.[23–26]

III. Results

Geometrical factors around Iso

The crystal structure of the WT *D. vulgaris* (Miyazaki F) FBP was determined by Suto *et al.*,[28] and those of the E13T and E13Q isomers by Nakanishi *et al.*[27] The corresponding MD structures of the WT, E13T, E13Q, W32Y and W32A isoforms of FBP are shown in Fig. 1, whilst Fig. 2 shows the time-dependent changes in the center-to-center distances (R_c) between Iso and Trp32, Tyr35 and Trp106 in the WT, E13T and E13Q isoforms, respectively. The distances between Iso and the Tyr32, between Iso and Tyr35 and between Iso and Trp106 in W32Y and between Iso and Tyr35 and between Iso and Trp106 in W32A, respectively, have already been reported.[23,24] Here, the WT FBP displayed long term fluctuations in the Rc values, in addition to the instantaneous fluctuation, while such long term fluctuation was not found in the E13T and E13Q isoforms.

The time-dependent changes in the edge-to-edge distances (R_e) between the donors and the Iso are shown in Fig. 3. The R_e fluctuation pattern was somewhat similar to that seen with the R_c values in the WT, E13T and E13Q FBP isoforms. The time-dependent changes in the inter-planar angles between the Iso residue and the indicated PET donor aromatic amino acids are shown in Fig. 4 for the WT, E13T and E13Q isoforms. The variation in the angles was highest in the WT, in accord with

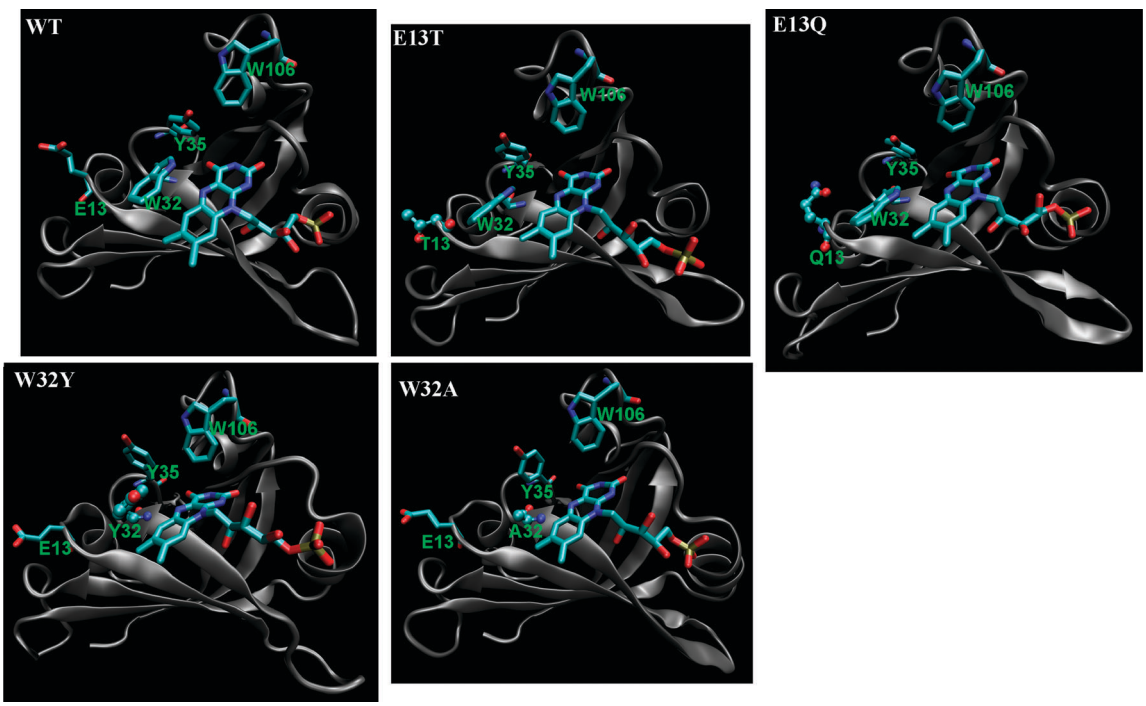

Fig. 1 Snapshots of five FBP systems (WT, E13T, E13Q, W32Y, W32A). Iso, Y35, W106 and amino acids at positions 13 and 32 are shown in stick models. WT, W32Y and W32A contain Glu13 while WT, E13T and E13Q contain Trp32, respectively.

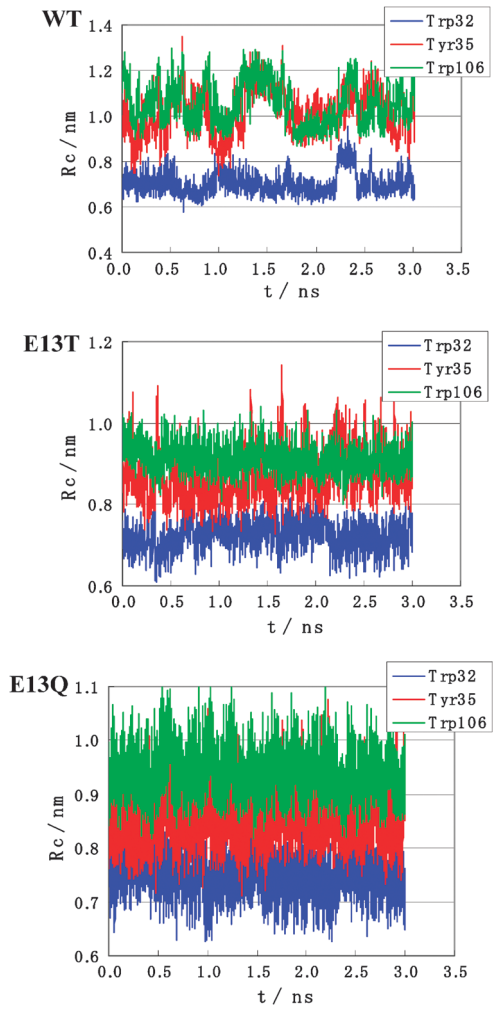

Fig. 2 Fluctuation of center-to-center distance between Iso and nearby aromatic amino acids in WT, E13T and E13Q. R_c denotes center-to-center distance. Trp32, Tyr35 and Trp106 in insets denote the R_c between Iso and these aromatic amino acids. Mean values of R_c are listed in Table 1.

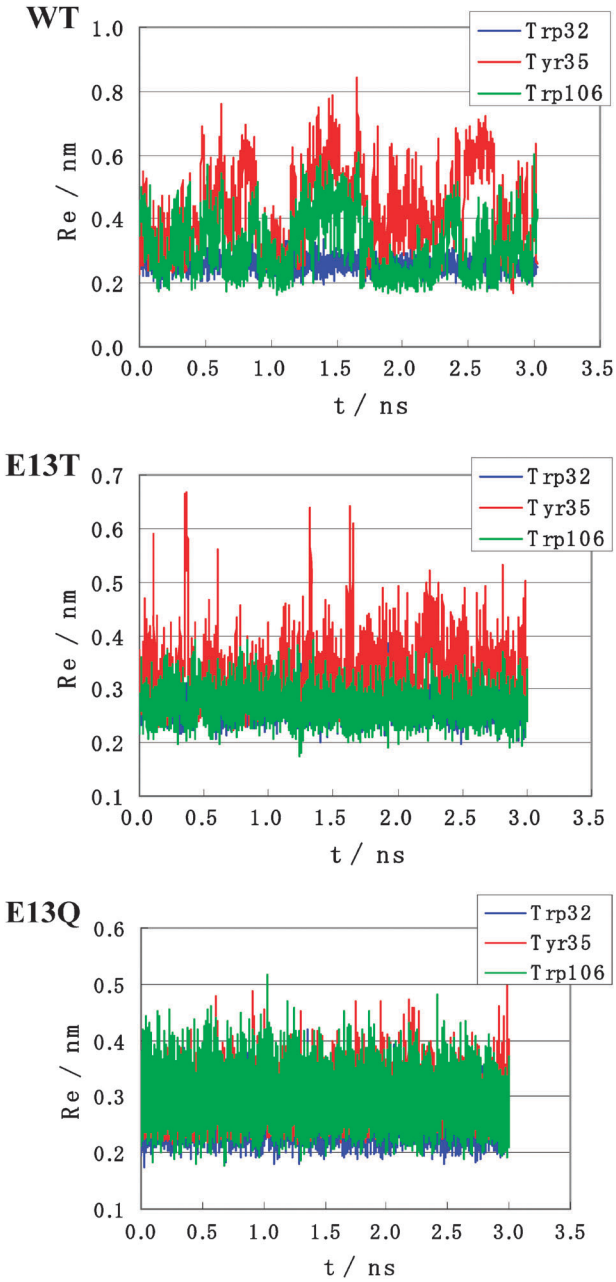

Fig. 3 Fluctuation of edge-to-edge distance between Iso and nearby aromatic amino acids. R_e denotes edge-to-edge distance. Trp32, Tyr35 and Trp106 in insets indicate R_e between Iso and these amino acids. Mean values of R_e are listed in Table 1.

the observed R_c and R_e data. The mean geometrical factors, averaged over the MD time range, are listed in Table 1. The mean R_c values between Iso and Trp32 were slightly higher in the E13T (1.03-fold) and E13Q (1.06-fold) isoforms than that for the WT, but was smaller (0.93-fold) between Iso and the Tyr32 residue in W32Y, which may be ascribed to the replacement of the Trp by the smaller Tyr residue. The R_c values between Iso and Tyr35 was shorter by 0.86-fold in E13T, by 0.84-fold in E13Q, by 0.81-fold in W32Y and by 0.76-fold in W32A, compared to the one in WT. In the W32A isoform the bulky Trp32 residue is replaced by the smaller Ala32, and so the Tyr35 might become closer to Iso. The R_c values between Iso and Trp106 were also shorter by 0.87-fold in E13T, by 0.89-fold in E13Q, by 0.86-fold in W32Y and by 0.85-fold in W32A, compared to the one in WT. These distances in the WT, E13T and E13Q isomers compare well with those obtained from the crystal structures. The R_c values between Iso and Trp32 in the crystals were 0.71 nm in all three FBP isomers, with values of 0.76–0.77 nm for the Iso-Tyr35 pair and 0.84–0.85 nm for the Iso-Trp106 pair.[27,28] In slight contrast, the R_c value for the Iso-Trp32 pair and Iso-Trp106 obtained by the MD here were 0.01–0.25 nm and 0.05–0.2 nm longer, respectively, than those obtained from the crystal structure.

The mean R_e values and the inter-planar angles between the donors and acceptor in all five FBP isoforms are also listed in Table 1. The inter-planar angles between Iso and Trp32 decreased from -52° in the WT by 9 and 14° (magnitude) in E13T and E13Q, respectively. The inter-planar angle between Iso and Tyr32 in W32Y increased by 81° compared to one in

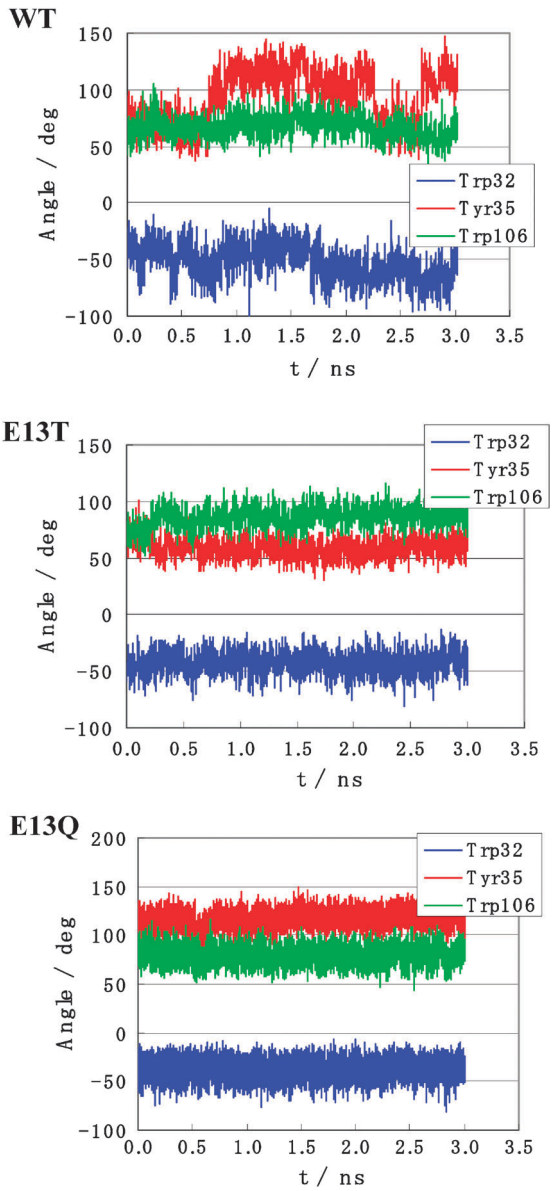

Fig. 4 Fluctuation of inter-plane angles between Iso and nearby aromatic amino acids. Trp32, Tyr35 and Trp106 in insets denote the inter-planar angles between Iso and these aromatic amino acids. Mean angles are listed in Table 1.

WT. In the W32Y isoform, Tyr32 may be quite flexible because of the smaller volume of Tyr compared to Trp. The extent of the fluctuation may be judged from the relative standard deviation (RSD) in Table 1, obtained as the SD/mean value. For all three parameters (R_c, R_e and inter-planar angle), the RSD values were highest in the WT, which implies that the WT protein structure fluctuates the most among the five FBP isomers.

Time-dependent changes in the distances between the amino acids at position 13 and the PET donors or acceptor in all five FBP isomers are shown in Fig. S1 (ESI† B). At a glance, the fluctuation of the distances was marked in the WT, E13Q and W32A isomers, compared to the E13T and W32Y ones. The mean distances between these amino acid residues at the 13th position and the Iso or the PET-donor aromatic amino acid residues are listed in Table 2. The mean distances from Glu13 to Trp32 (0.92–0.98 nm) were fairly uniform across the WT, W32Y and W32A isoforms compared to that for Glu13 to Iso (1.49–1.64 nm), Tyr35 (0.99–1.46 nm) and, especially, Trp106 (1.72–2.13 nm). Indeed, the variations in the distances, as judged from the SD values, were pronounced for residue 13 to Tyr35 and Trp106, compared to those for residue 13 to Iso and Trp32.

Fluorescence dynamics

The fluorescence decays of the five FBP isomers were simultaneously analyzed using both MH and KM theories *via* Method A. For the MH theory based analysis (Fig. 5), agreements between the observed and calculated decays were quite good in the WT, W32A and W32Y isoforms, but not so good in E13T and E13Q isoforms, especially at the long tails. For the KM theory based analysis (Fig. 6), agreements between the observed and calculated decays were quite good for the WT, E13T, E13Q and W32Y isoforms, but very poor in the W32A isoform. Thus, both the MH and KM theories did not reproduce well the single exponential decay of W32A.

The observed fluorescence decays of the WT, E13T and E13Q FBP isomers were also analyzed with both MH and KM theories using the alternative Method B. The values of chi-square were $\chi_5^2 = 5.66 \times 10^{-3}$ by Method A and $\chi_3^2 = 9.81 \times 10^{-3}$ by Method B with MH theory, and $\chi_5^2 = 2.49 \times 10^{-3}$ by Method A and $\chi_3^2 = 1.86 \times 10^{-3}$ by Method B with KM theory. The agreements between the observed and calculated decays were better with the KM theory by both Methods A and B than with the MH theory.

PET parameters

Best-fit PET parameters with MH theory and KM theory obtained by Method A and Method B are listed in Table 3. The values of H_{Trp} were 0.015 eV by Method A, and 0.010 eV by Method B and those of H_{Tyr} were 0.00561 eV by Method A, and 0.002 eV by Method B with MH theory. These values did not differ much between the two methods. ε_0^{DA} is influential on ET rate through solvent reorganization energy λ_S^{jk} given by eqn (2) and ES, energy between a PET donor and acceptor, $-e^2/\varepsilon_0^{DA}R_{jk}$, in eqn (1) and (4). ε_0^{DA} was obtained as 3.33 with MH theory by Method A, and 2.36 by Method B. ε_0^{DA} was obtained to be 2.19 with KM theory by Method A, and 2.23 by Method B. ε_0^j (j = WT, E13T, E13Q, W32Y and W32A with Method A, j = WT, E13T, E13Q with Method B) are influential upon ET rate through $ES_j(k)$ in eqn (5) and (6). Dielectric constants determined with MH theory were $\varepsilon_0^{WT} = 5.81$, $\varepsilon_0^{E13T} = 5.82$, $\varepsilon_0^{E13Q} = 4.83$, $\varepsilon_0^{W32Y} = 13.0$ and $\varepsilon_0^{W32A} = 13.0$ by Method A, and $\varepsilon_0^{WT} = 8.34$, $\varepsilon_0^{E13T} = 7.57$, $\varepsilon_0^{E13Q} = 6.00$ by Method B. In the analysis with KM theory, PET parameters related to the electronic interaction part were taken from the previous work,[27] ν_0^q (q = Trp, 1016 ps^{-1}; q = Tyr, 197 ps^{-1}), β^q (Trp, 21.0 nm^{-1}; Tyr, 6.25 nm^{-1}), and R_0^q (Trp, 0.663 nm; Tyr, 0.499 nm). Dielectric constants determined with KM theory were $\varepsilon_0^{WT} = 14.8$, $\varepsilon_0^{E13T} = 5.99$, $\varepsilon_0^{E13Q} = 6.69$, $\varepsilon_0^{W32Y} = 5.89$ and $\varepsilon_0^{W32A} = 6.29$ by Method A, and $\varepsilon_0^{WT} = 5.82$, $\varepsilon_0^{E13T} = 4.39$, and $\varepsilon_0^{E13Q} = 4.82$ by Method B.

Table 1 Geometrical factors related to Iso and the indicated aromatic amino acids (PET donors) in the five FBP isomers[a]

	R_c[b]/nm				R_e[b]/nm				Inter-planar angle/°			
Protein system	Trp32	Tyr32	Tyr35	Trp106	Trp32	Tyr32	Tyr35	Trp106	Trp32	Tyr32	Tyr35	Trp106
WT	0.703	—	1.016	1.052	0.261	—	0.425	0.314	−52.2	—	93.3	67.4
(RSD[c])	(0.072)	—	(0.097)	(0.088)	(0.086)	—	(0.292)	(0.290)	(−0.3)	—	(0.3)	(0.1)
E13T	0.724	—	0.872	0.913	0.269	—	0.331	0.269	−42.5	—	59.3	85.7
(RSD[c])	(0.048)	—	(0.069)	(0.038)	(0.079)	—	(0.181)	(0.111)	(−0.2)	—	(0.2)	(0.1)
E13Q	0.748	—	0.854	0.939	0.265	—	0.287	0.294	−37.8	—	116.4	79.2
(RSD[c])	(0.044)	—	(0.053)	(0.043)	(0.095)	—	(0.123)	(0.131)	(−0.2)	—	(0.1)	(0.1)
W32Y	—	0.654	0.826	0.907	—	0.276	0.284	0.251	—	28.7	76.7	77.5
(RSD[c])	—	(0.050)	(0.075)	(0.036)	—	(0.091)	(0.167)	(0.110)	—	(0.6)	(0.1)	(0.1)
W32A	—	—	0.769	0.895	—	—	0.290	0.277	—	—	42.8	70.9
(RSD[c])	—	—	(0.082)	(0.050)	—	—	(0.226)	(0.139)	—	—	(0.6)	(0.1)

[a] Mean values of the factors between Iso and the nearby indicated aromatic amino acids are listed. The mean values were obtained by taking an average over the entire MD time range. [b] Centre-to-centre (R_c) and edge-to-edge (R_e) distances. [c] Relative standard deviation (RSD), obtained from SD/mean value.

Table 2 Mean distance between the 13th amino acid residue and the indicated aromatic amino acids (chromophores) in the five FBP isomers[a]

System	Iso	Trp32	Tyr32	Tyr35	Trp106
WT[b]	1.53 ± 0.10	0.98 ± 0.09	—	0.99 ± 0.16	1.72 ± 0.15
E13T[c]	1.49 ± 0.06	0.92 ± 0.07	—	1.22 ± 0.08	1.97 ± 0.09
E13Q[c]	1.58 ± 0.13	0.98 ± 0.12	—	1.12 ± 0.16	1.84 ± 0.17
W32Y[b]	1.64 ± 0.07	—	1.13 ± 0.08	1.46 ± 0.09	2.13 ± 0.09
W32A[b]	1.60 ± 0.11	—	—	1.24 ± 0.15	1.76 ± 0.16

[a] Mean distances (+1 standard deviation), averaged over the MDS time range, are shown in units of nm. [b] Distances were obtained taking the average over all distances between atoms in the aromatic ring and the center of the two oxygen atoms in the side chain of Glu13. [c] Obtained by taking the average over all distances between the atoms in the aromatic ring and the oxygen atom of the Thr13 (E13T) or Gln13 (E13Q) side chain.

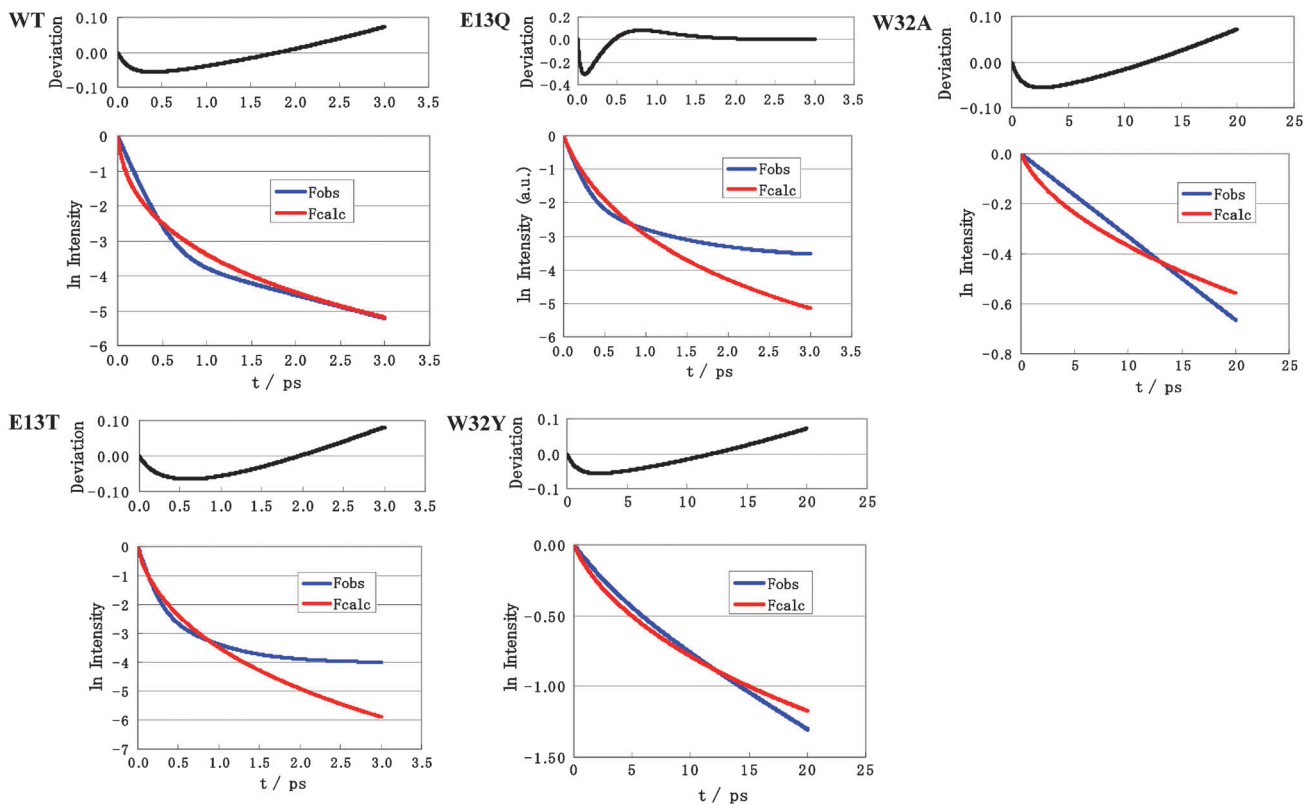

Fig. 5 Fluorescence decays of five FBP systems obtained by MH theory. F_{obs} and F_{calc} in insets denote the observed and calculated fluorescence decays. The five calculated decays were obtained with ET parameters using MH theory by Method A. Best-fit ET parameters are listed in Table 3. Upper panel of each decay represents deviation between the observed and calculated decays given by eqn (15).

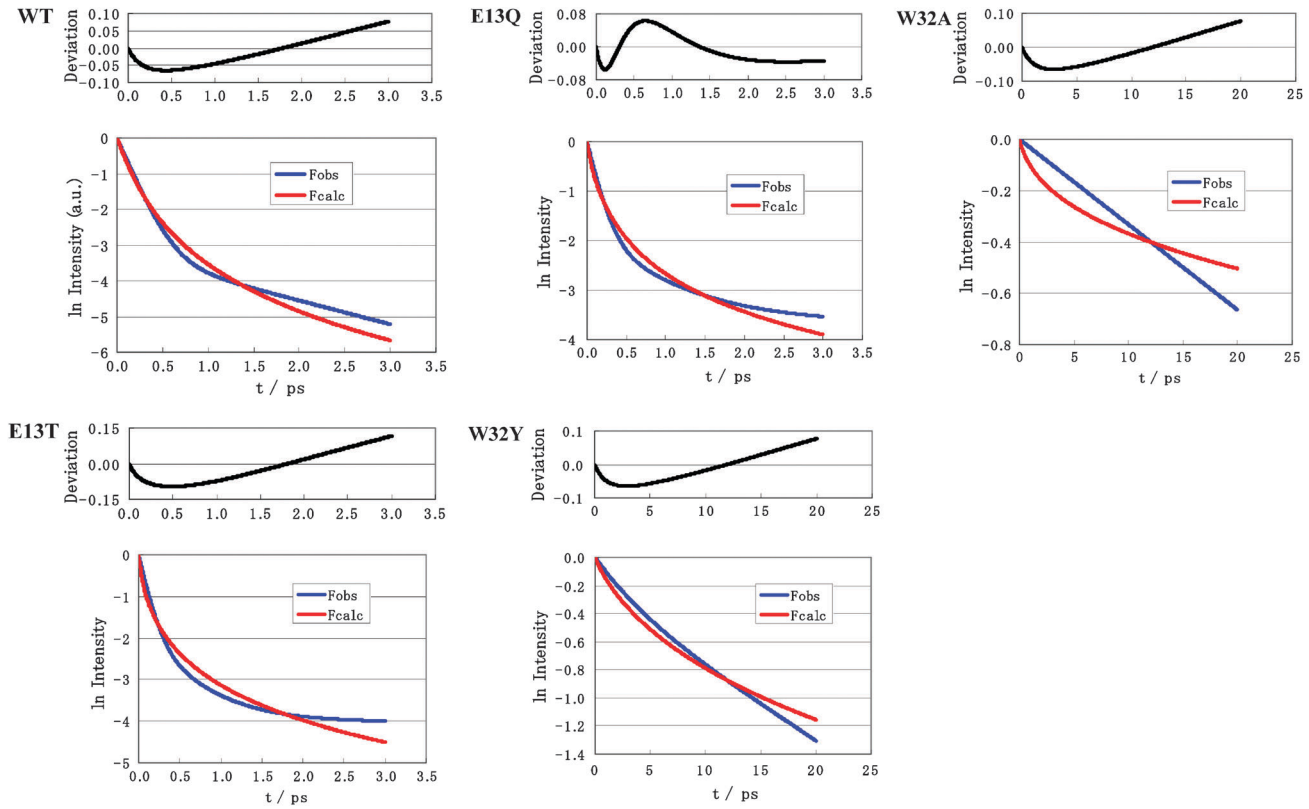

Fig. 6 Fluorescence decays of five FBP systems obtained by KM theory. F_{obs} and F_{calc} in insets denote the observed and calculated fluorescence decays. The five calculated decays were obtained with best-fit ET parameters using KM theory by Method A. The best-fit ET parameters are listed in Table 3. Upper panels of the decays represent deviations between the observed and calculated decays given by eqn (15).

Table 3 PET parameters obtained using the MH and KM theories

			FBP isomer					Overall				
Theory	Method		WT	E13T	E13Q	W32Y	W32A	ε_0^{DA}	G_{Iso}/eV	H_{Trp}/eV	H_{Tyr}/eV	Chi-square[c]
MH[a]	A	ε_0^j	5.81	5.82	4.83	13.0	13.0	3.33	10.3	0.015	0.00561	—
		χ_j^{2b}	7.04×10^{-3}	6.59×10^{-3}	1.09×10^{-2}	1.59×10^{-3}	2.17×10^{-3}	—	—	—	—	χ_5^2 5.66×10^{-3}
	B	ε_0^j	8.34	7.57	6.00	—	—	2.36	8.41	10	2.0	—
		χ_j^{2b}	1.97×10^{-2}	4.47×10^{-3}	5.30×10^{-3}	—	—	—	—	—	—	χ_3^{2d} 9.81×10^{-3}
KM[e]	A	ε_0^j	14.8	5.99	6.69	5.89	6.29	2.19	6.71	—	—	—
		χ_j^{2b}	1.25×10^{-3}	2.49×10^{-3}	2.09×10^{-3}	1.89×10^{-3}	4.45×10^{-3}	—	—	—	—	χ_5^2 2.49×10^{-3}
	B	ε_0^j	5.82	4.39	4.82	—	—	2.23	6.88	—	—	—
		χ_j^{2b}	1.19×10^{-3}	2.53×10^{-3}	1.88×10^{-3}	—	—	—	—	—	—	χ_3^2 1.86×10^{-3}
	C[f]	ε_{00}^j	8.03	5.19	4.67	—	—	—	9.22	—	—	—

[a] PET rate is given by eqn (1). The meaning of the PET parameters is described below and in eqn (1). [b] χ_j^2 (j = WT, E13T, E13Q, W32Y and W32A by Method A, j = WT, E13T and E13Q by Method B) is defined by eqn (14). [c] χ_5^2 is defined by eqn (16). [d] χ_3^2 is defined by eqn (17). [e] The PET rate is given by eqn (4). The meaning of the PET parameters are described below eqn (4). PET parameters related to the electronic interaction part were taken from the reported values,[27] ν_0^q (q = Trp, 1016 ps^{-1}; q = Tyr, 197 ps^{-1}), β^q (Trp, 21.0 nm^{-1}; Tyr, 6.25 nm^{-1}) and R_0^q (Trp, 0.663 nm; Tyr, 0.499 nm). [f] The PET parameters are taken from a previous report determined from the crystal structures of WT, E13T and E13Q.[27] In this method the value of ε_0^{DA} was assumed to be equal to one of ε_0^j in respective system j (j = WT, E13T and E13Q).

The dielectric constants reported with X-ray structures of WT, E13T and E13Q[27] were also listed in Table 3 for comparison (Method C), $\varepsilon_0^{WT} = 8.03$, $\varepsilon_0^{E13T} = 5.19$, and $\varepsilon_0^{E13Q} = 4.67$, where KM theory was used. The values of ε_0^{DA} were always less than ε_0^j. This is reasonable because amino acid rarely exists between the donors and acceptor, while many amino acids exist between the Iso anion or PET donor cations and ionic groups in the proteins.

The values of G_{Iso}^0, which should be related to electron affinity of Iso*, were 10.3 eV by Method A, and 8.41 eV by Method B with MH theory. The values of G_{Iso}^0 were 6.71 eV by Method A, and 6.88 eV by Method B with KM theory.

G^0_{Iso} may be dependent on the environment around Iso in each protein, including hydrogen bondings.

PET rate

Fig. 7 shows the time-dependent PET rates calculated using KM theory by Method A. In the WT, E13T and E13Q isoforms the PET rates were fastest from Trp32, whilst in the W32Y isoform the PET rate was fastest from Trp106, followed by Tyr32 and Tyr35. This is in agreement with previous observations that the PET rate from Tyr is always slower than that from Trp.[23,24,27,36] The mean PET rates obtained in this study over the MD time range are listed in Table 4. The rate for Trp32 ranged from 7.1 ps^{-1} in the WT to 17.2 ps^{-1} in E13T, whilst that for Tyr32 (in W32Y) was much slower (1.6×10^{-7} ps^{-1}). The PET rates from Trp106 were 0.192 ps^{-1} in W32Y and 0.176 ps^{-1} in W32A.

ES energy

The time-evolution of ES energies, as expressed by eqn (5), is shown in Fig. S2 (ESI† B), where the ES energies of the Tyr35 cation were always positive. For the WT, the ES energies were also positive for the Iso anion, but negative in the Trp106. The ES energies for Trp106 were likewise negative in the E13T and E13Q isoforms, but positive in W32Y and W32A, whilst that for Trp32 was positive in all four single substitution isoforms but fluctuating around zero in the WT. However, whilst the ES energies for Iso in W32A and W32Y were positive, as in the WT, it fluctuated around zero in both the E13T and E13Q isoforms. The difference in the ES energies between the WT and E13T or E13Q isoforms may be ascribed to the disappearance of the negatively charged Glu13 residue in the E13T and E13Q FBP isomers. Every ES energy in W32Y and W32A was always positive, and quite different from the WT, E13T and E13Q FBP isoforms.

The time-evolution of the net ES energies, as expressed by eqn (6), is shown in Fig. 8. The net ES energies of Trp32 and Tyr35 cations were always positive in all systems, whilst those for Trp106 were negative in WT, E13T and E13Q, but positive in W32Y and W32A.

Mean ES energies over MD time range are listed in Table 4. Mean ES energies of the Iso anion were 0.071 eV in WT, −0.023 eV in E13T, 0.021 eV in E13Q, 0.074 eV in W32Y and 0.079 eV in W32A. Mean ES energies of the Trp32 cation were

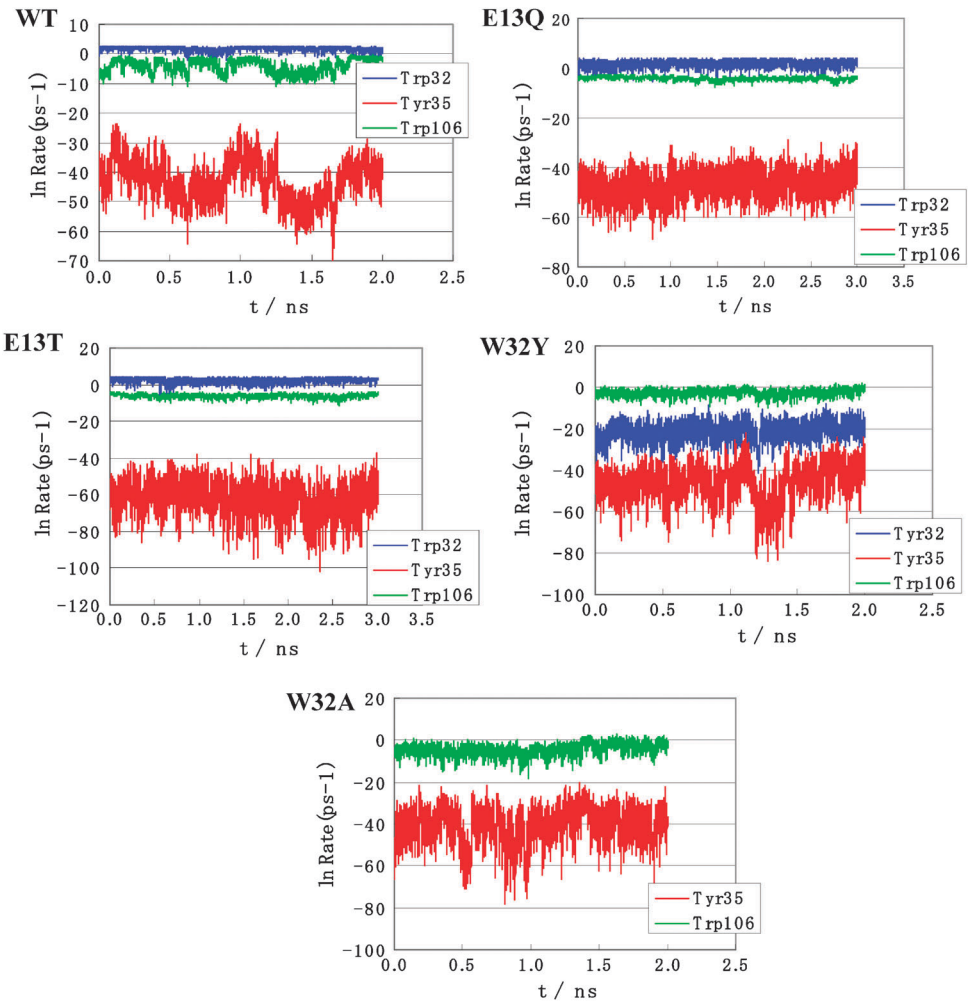

Fig. 7 ET rates from aromatic amino acids to Iso*. ET rate is expressed in units of ps^{-1}. Insets show the aromatic amino acids of ET donors. ET rates in units of ps^{-1} were obtained by ET parameters with KM theory by Method A.

Table 4 Physical quantities related to the PET rate[a]

Quantity		WT	E13T	E13Q	W32Y	W32A
k_{KM}^{jk} [b]/ps^{-1}	Trp32	7.10 ± 3.08	17.22 ± 14.76	10.81 ± 10.43	—	—
	Tyr32	—	—	—	$1.6 + 30 \times 10^{-7}$	
	Tyr35	$4 \pm 95 \times 10^{-14}$	$6.4 \pm 400 \times 10^{-21}$	$7 \pm 200 \times 10^{-17}$	$3.7 \pm 200 \times 10^{-14}$	$5 \pm 130 \times 10^{-13}$
	Trp106	0.082 ± 0.110	0.003 ± 0.003	0.018 ± 0.011	0.192 ± 0.350	0.176 ± 0.599
λ_S^{jk}[c] (eV)	Trp32	0.202 ± 0.005	0.206 ± 0.004	0.208 ± 0.004	—	—
	Tyr32	—	—	—	0.217 ± 0.005	—
	Tyr35	0.249 ± 0.006	0.240 ± 0.005	0.229 ± 0.004	0.236 ± 0.006	0.231 ± 0.006
	Trp106	0.232 ± 0.005	0.223 ± 0.003	0.225 ± 0.003	0.223 ± 0.002	0.222 ± 0.003
$E_j(k)$[d] (eV)	Iso	0.071 ± 0.013	−0.023 ± 0.024	0.021 ± 0.028	0.074 ± 0.030	0.079 ± 0.026
	Trp32	0.005 ± 0.017	0.335 ± 0.043	0.269 ± 0.032	—	—
	Tyr32	—	—	—	0.123 ± 0.033	
	Tyr35	0.080 ± 0.025	0.472 ± 0.050	0.391 ± 0.041	0.256 ± 0.052	0.242 ± 0.052
	Trp106	−0.140 ± 0.007	−0.326 ± 0.011	−0.297 ± 0.010	0.141 ± 0.039	0.230 ± 0.054
$ES_j(k)$[e] (eV)	Trp32	0.076 ± 0.010	0.312 ± 0.027	0.290 ± 0.021	—	—
	Tyr32	—	—	—	0.197 ± 0.020	—
	Tyr35	0.150 ± 0.022	0.449 ± 0.041	0.412 ± 0.035	0.330 ± 0.046	0.321 ± 0.043
	Trp106	−0.069 ± 0.017	−0.349 ± 0.025	−0.276 ± 0.029	0.215 ± 0.034	0.309 ± 0.042
$-e^2/\varepsilon_0^{DA} R_{jk}$[f] (eV)	Trp32	−0.949 ± 0.055	−0.912 ± 0.045	−0.883 ± 0.045	—	—
	Tyr32	—	—	—	−1.009 ± 0.049	—
	Tyr35	−0.660 ± 0.070	−0.759 ± 0.051	−0.883 ± 0.039	−0.803 ± 0.039	−0.863 ± 0.066
	Trp106	−0.627 ± 0.056	−0.722 ± 0.027	−0.703 ± 0.030	−0.728 ± 0.027	−0.728 ± 0.037
$-\Delta G_T^0$[g] (eV)	Trp32	0.371	0.098	0.090	—	—
	Tyr32	—	—	—	−0.491	—
	Tyr35	−0.792	−0.992	−0.832	−0.829	−0.760
	Trp106	0.194	0.569	0.477	0.011	−0.073

[a] Mean (+1 standard deviation) physical quantities obtained with KM theory by Method A were obtained taking an average over the entire MDS time range. [b] k_{KM}^{jk} is given by eqn (4). j = WT, E13T, E13Q, W32Y and W32A. k = 1 for Trp32 (Tyr32 in W32Y), 2 for Tyr35 and 3 for Trp106. [c] Solvent reorganization energy given by eqn (2). The meaning of j and k are indicated in footnote b. [d] $E_j(k)$ is given by eqn (5). The meaning of j and k are indicated in footnote b. [e] Net ES energy given by eqn (6). The meanings of j and k are indicated in footnote b. [f] ES energy between a donor and acceptor. ε_0^{DA} is static dielectric constant in the domain between the donors and acceptor, and R_{jk} is the center-to-center distance between Iso and the indicated ET donor. The meaning of j and k is indicated in footnote b. [g] Total free energy gap, given by eqn (19).

0.005 eV in WT, 0.335 eV in E13T, 0.269 eV in E13Q. In W32Y the ES energy of the Tyr32 cation was 0.123 eV. ET rate depends on net ES energy (see eqn (1), (4) and (6)). Mean net ES energies of Trp32 were 0.076 eV in WT, 0.312 eV in E13T, 0.290 eV in E13Q. In W32Y the net ES energy of Tyr32 was 0.197 eV. Mean net ES energies of Trp106 were −0.069 eV in WT, −0.349 eV in E13T, −0.276 eV in E13Q, 0.141 eV in W32Y and 0.230 eV in W32A.

Time-dependent changes in ES energies between ET donor cations and acceptor anion are shown in Fig. S3 (ESI† B). The mean ES energies are also listed in Table 4. The energies between the Iso anion and Trp32 cation were −0.949 eV in WT, −0.912 eV in E13T, −0.883 eV in E13Q. The ES energy between the Iso anion and Tyr32 cation was −1.009 eV in W32Y. The energy of Trp32 was greatest in magnitude among three ET donors, because R_c between Trp32 and Iso was shortest.

Solvent reorganization energy

The solvent reorganization energy of the PET donor k in FBP j (λ_S^{jk}) is expressed by eqn (2), and the time-dependent changes in λ_S^{jk} are shown in Fig. S4 (ESI† B). λ_S^{jk} mostly depends on R_{jk}, because the other quantities in eqn (2) are time-independent, including ε_0^{DA}. The mean values of λ_S^{jk} are listed in Table 4, where for Trp32 essentially the same value (0.202–0.208 eV) was seen in the WT, E13T and E13Q isoforms, but that for Tyr32 in W32Y was slightly higher (0.217 eV). Indeed, across all four PET donors (Trp32, Tyr232, Tyr 35 and Trp106) these values did not change much (0.2–0.25 eV).

Energy gap law. Normal energy gap law is expressed by eqn (18).

$$\ln k_{KM}^{jk} \propto (-\Delta G_T^0 + \lambda_S^{jk})^2 \quad (18)$$

Here the total free energy gap ($-\Delta G_T^0$) is given by eqn (19).

$$-\Delta G_T^0 = -\Delta G_q^0 + e^2/\varepsilon_0^{DA} R_{jk} - ES_j(k) \quad (19)$$

If λ_S^{jk} varies much with the PET donor, then the following modified energy gap law may be useful.

$$(\ln k_{KM}^{jk})/\lambda_S^{jk} \propto (-\Delta G_T^0/\lambda_S^{jk} + 1)^2. \quad (20)$$

Fig. 9 shows the energy gap laws obtained with all five of the FBP isomers, with the required numerical data being summarized in Table 4. Fig. 9A shows a normal energy gap law, and Fig. 9B the modified energy gap law. In both cases, the obtained data with KM theory were expressed well by parabolic functions, being $Y = -35.24X^2 + 11.34X - 0.266$ for the normal energy gap law, where Y is nk_{KM}^{jk} and X is $-\Delta G_T^0$, and $Y = -9.45X^2 + 8.57X + 8.89$ for the modified energy gap law, where Y is $(nk_{KM}^{jk})/\lambda_S^{jk}$ and X is $-\Delta G_T^0/\lambda_S^{jk}$. Variation in λ_S^{jk} was not significant because the ε_0^{DA} values used were common among the PET donors and FBP isoforms, and accordingly an excellent parabolic function was obtained with the normal energy gap law. The PET in these FBP isoforms mostly took

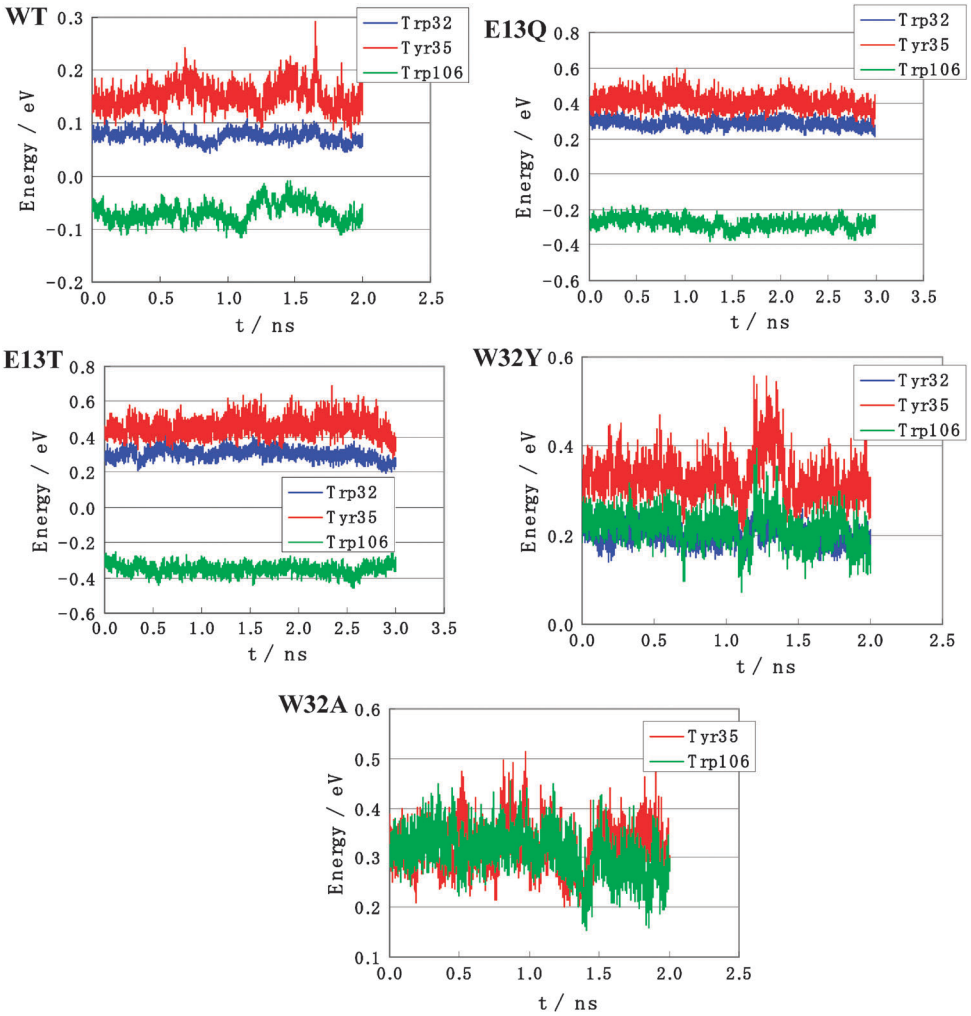

Fig. 8 Time-dependent change in net ES energy. Net ES energies (eqn (6)) were calculated with KM theory by Method A. Amino acids in insets indicate ET donors.

place in the normal region. The value of $-\Delta G^0_T$ at the maximum rate was *ca.* 0.2 eV.

IV. Discussion

In the present work the observed ultrafast fluorescence dynamics of five FBP systems were analyzed both with MH theory and KM theory based on their MD structures. The calculated decays better described the observed ones with KM theory than with MH theory, despite that both the theories are similar except for the $1 + \exp\{\beta^q(R_{jk} - R^q_0)\}$ term in KM theory (see eqn (1) and (4)). This term becomes important in a non-adiabatic ET process at $R_{jk} > R^q_0$. This may be the reason why KM theory can describe better the observed fluorescence dynamics compared to MH theory.

Here the dielectric constant of the domain between the donors and Iso (ε_0^{DA}) was determined separately from those of the other domains in the proteins, ε_0^j (j = WT, E13T, E13Q, W32Y and W32A) for the first time, because amino acids rarely exist in the region between the donors and acceptor, whereas many amino acids exist in the domain between the PET products and ionic groups in the proteins. Actually, the values of ε_0^{DA} were always less than those of ε_0^j when the analysis was performed using either MH or KM theories with either Method A or B (Table 3). The $ES_j(k)$ values were found to depend significantly on the dielectric constant (ε_0^j), which can vary from 1 in vacuum to 78 in water. The mean values of ε_0^j were 8.7, 5.9 and 5.6 in the WT, E13T and E13Q isoforms, respectively, obtained by both Methods A and B with both MH and KM theories, and 9.4 and 9.6 in the W32Y and W32A, respectively, obtained by analysis using Method A with either MH or KM theories. The dielectric constants of the WT, E13T and E13Q isoforms obtained from the X-ray structures and the average fluorescence lifetimes[27] (Method C in Table 3) were quite close to those obtained in the present work based upon the MD structures and the fluorescence dynamics. The dielectric constant values did not differ much among the WT (8.7), W32Y (9.4) and W32A (9.6), but those of the E13T and E13Q isoforms were 1.6-fold and 1.7-fold lower than the WT, respectively. These results are reasonable because the E13T and E13Q isoforms have one negative charge missing compared to the WT.

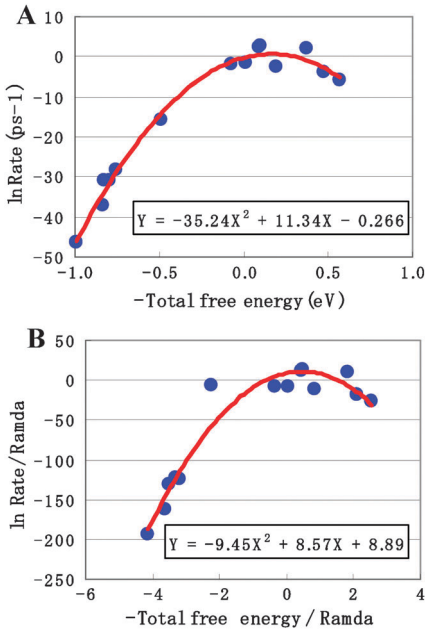

Fig. 9 Energy gap law in all FBP systems. Labels of vertical and horizontal axes indicate nk_{KM}^{jk} and $-\Delta G_T^0$ in A, and $nk_{KM}^{jk}/\lambda_S^{jk}$ and $-\Delta G_T^0/\lambda_S^{jk}$ in B, respectively. k_{KM}^{jk} is expressed in unit of ps^{-1}, and $-\Delta G_T^0$ in unit of eV. Solid lines denote approximate 2nd order polynomials, where Y and X are nk_{KM}^{jk} and $-\Delta G_T^0$ in A, and $nk_{KM}^{jk}/\lambda_S^{jk}$ and $-\Delta G_T^0/\lambda_S^{jk}$ in B, respectively.

It is important to consider which PET parameters are most influential upon the PET rate. The effect of variation in the pre-exponential factors may be not very important in terms of influencing the PET rates when determined by both MH and KM theories. Among the parameters in the exponential functions, the effect of variation in the reorganization energy (λ_S^{jk}) on the PET rates could have been suppressed because of the occurrence of λ_S^{jk} in the denominator. In the present method the values of λ_S^{jk} did not vary much between the different PET donors, because λ_S^{jk} in eqn (2) depends only on the donor–acceptor distance, R_{jk}, whereas in the former method[25,26] λ_S^{jk} depends on both R_{jk} and dielectric constant in proteins. Actually λ_S^{jk} in Table 4 varied from 0.202 eV (Trp32 in WT) to 0.249 eV (Tyr35 in WT). It is not unreasonable to presume that the total free energy gap, as given by eqn (19), is the most influential factor upon the PET rates. $ES_f(k)$ greatly varied with the PET donor, from −0.349 eV (Trp106 in E13T; PET rate 17.22 ps^{-1} was fastest among the all donors) to 0.449 eV (Tyr35 in E13T; PET rate 6.4×10^{-21} ps^{-1} was slowest), whilst those for $-\Delta G_q^0$ (q = Trp or Tyr) varied at most 0.8 eV, and furthermore the ES energy between the donor and acceptor molecules ($-e^2/\varepsilon_0^{DA}R_{jk}$) did from −1.009 eV (Tyr32 in W32Y) to −0.627 eV (Trp106 in WT). It may be concluded that $ES_f(k)$ is the most influential factor for PET rate in FBP systems.

According to Yoshimori *et al.*[37] the energy gap law becomes asymmetric along $-\Delta G_T^0$, when the effect of the electronic polarizability of solute and solvent molecules is not negligible. In the present work we have used classical KM theory in which a non-linear response due to dielectric saturation was not taken into account. Hence, the logarithm of the PET rates obtained in this analysis could be approximated to be a parabolic function of $-\Delta G_T^0$. The energy gap law in proteins was first demonstrated in the reaction center of the purple bacterium, *Rhodobacter sphaeroides*, by Gunner and Dutton,[38] and the plant photosystem I and in the reaction center of the purple bacterium by Iwaki *et al.*[39] In these systems the PET takes place in the normal regions. Turro *et al.*[40] demonstrated that PET in a homologous series of the excited RuII diimines with cytochrome (cyt) *c* in its oxidized and reduced forms takes place in both normal region and the inverted region. In the FBP systems, the PET also took place both in the normal region and in the inverted region. At the optimal rates the free energy driving forces, $-\Delta G_T^0$, were 0.2 eV in photosystem I,[39] 0.7 eV in the reaction center of the purple bacterium,[39] the excited RuII diimine complexes—FeIIcyt *c*, 0.8 eV,[40] and the excited RuII diimine complexes—FeIIIcyt *c*, 0.9 eV.[40] In the FBP isomers it was found to be 0.2 eV (Fig. 9).

Fluctuation in the ET rates from Tyr to the excited flavin in a single molecule of flavin reductase has been observed in the time domain of sub-milliseconds to seconds.[41] Fluctuation in the ET rate in the NAD(P)H : flavin oxidoreductase complex was also computationally investigated.[42] Dutton law in which ET rate expressed as an exponentially decreasing function of the donor–acceptor distance was theoretically examined from the point of view of the donor–acceptor distance fluctuation.[43] In these works the fluctuation in ET rates was interpreted in terms solely of the donor–acceptor distance. Electrostatic energy in the proteins is also an important factor for the ET rate. Fluctuation in the ES energy in the proteins may also contribute to the fluctuation of the ET rate, in addition to the donor–acceptor distance.

The PET mechanism may be related in some extent to the dark electron transfer mechanism in flavoproteins. Static dielectric constant and electrostatic energies in the proteins obtained by PET analysis may be used for the electron transfer rate without light, which should also play a very important role on the dark electron transfer reactions.

Acknowledgements

The Ratchadaphiseksomphot Endowment Fund is acknowledged for financial support. The authors would like to acknowledge the Computational Chemistry Unit Cell, Chulalongkorn University and the National Center for National Nanotechnology Center (NECTEC) for the use of computing facilities. The National Center of Excellence for Petroleum, Petrochemicals, and Advanced Materials (NCE-PPAM) is also acknowledged.

References

1 A. M. Kuznetsov and J. Ulstrup, *Electron Transfer in Chemistry and Biology: An Introduction to the Theory*, Wiley Series in Theoretical Chemistry, John Wiley & Sons, Ltd., New York, 1999.
2 *Advances in Chemical Physics*, ed. J. Jortner and M. Bixon, Electron Transfer—From Isolated Molecules to Biomolecules, Wiley-Interscience, New York, 1999, vol. 106.
3 R. E. Blankenship, *Molecular Mechanisms of Photosynthesis*, Wiley-Blackwell, New York, 2002.
4 A. Möglich, X. Yang, R. A. Ayers and K. Moffat, *Annu. Rev. Plant Biol.*, 2010, **61**, 21–47.

5 S. Masuda and S. C. E. Bauer, *Cell*, 2002, **110**, 613–623.
6 Y. Shibata, Y. Murai, Y. Satoh, Y. Fukushima, K. Okajima, M. Ikeuchi and S. Itoh, *J. Phys. Chem. B*, 2009, **113**, 8192–8198.
7 G. Weber, *Biochem. J.*, 1950, **47**, 114–118.
8 D. B. McCormick, *Photochem. Photobiol.*, 1977, **26**, 169–182.
9 P. A. van der Berg and A. J. W. G. Visser, in *New Trends in Fluorescence Spectroscopy Applications to Chemical and Life Sciences*, ed. B. Valeur and J. C. Brochon, Springer, Berlin, 2001, pp. 457–485.
10 N. Mataga, H. Chosrowjan, Y. Shibata and F. Tanaka, *J. Phys. Chem. B*, 1998, **102**, 7081–7084.
11 N. Mataga, H. Chosrowjan, Y. Shibata, F. Tanaka, Y. Nishina and K. Shiga, *J. Phys. Chem. B*, 2000, **104**, 10667–10677.
12 N. Mataga, H. Chosrowjan, S. Taniguchi, F. Tanaka, N. Kido and M. Kitamura, *J. Phys. Chem. B*, 2002, **106**, 8917–8920.
13 F. Tanaka, H. Chosrowjan, S. Taniguchi, N. Mataga, K. Sato, Y. Nishina and K. Shiga, *J. Phys. Chem. B*, 2007, **111**, 5694–5699.
14 H. Chosrowjan, S. Taniguchi, N. Mataga, F. Tanaka, D. Todoroki and M. Kitamura, *J. Phys. Chem. B*, 2007, **111**, 8695–8697.
15 H. Chosrowjan, S. Taniguchi, N. Mataga, F. Tanaka, D. Todoroki and M. Kitamura, *Chem. Phys. Lett.*, 2008, **462**, 121–124.
16 A. Karen, N. Ikeda, N. Mataga and F. Tanaka, *Photochem. Photobiol.*, 1983, **37**, 495–502.
17 A. Karen, M. T. Sawada, F. Tanaka and N. Mataga, *Photochem. Photobiol.*, 1987, **45**, 49–54.
18 D. P. Zhong and A. H. Zewail, *Proc. Natl. Acad. Sci. U. S. A.*, 2001, **98**, 11867–11872.
19 J. Pan, M. Byrdin, C. Aubert, A. P. M. Eker, K. Brettel and M. H. Vos, *J. Phys. Chem. B*, 2004, **108**, 10160–10167.
20 (*a*) R. A. Marcus, *J. Chem. Phys.*, 1956, **24**, 966–978; (*b*) R. A. Marcus, *Annu. Rev. Phys. Chem.*, 1964, **15**, 155–196; (*c*) C. Moser, J. Keske, K. Warncke, R. Farid and P. Dutton, *Nature*, 1992, **355**, 796–801.
21 (*a*) M. Bixon and J. Jortner, *J. Phys. Chem.*, 1991, **95**, 1941–1944; (*b*) M. Bixon and J. Jortner, *J. Phys. Chem.*, 1993, **97**, 13061–13066; (*c*) M. Bixon, J. Jortner, J. Cortes, H. Heitele and M. E. Michel-Beyerle, *J. Phys. Chem.*, 1994, **98**, 7289–7299.
22 (*a*) T. Kakitani, A. Yoshimori and N. Mataga, in *Advances in Chemistry Series*, ed. J. R. Bolton, N. Mataga and G. McLendon, American Chemical Society, Washington, DC, 1991, vol. 228, pp. 45–69; (*b*) T. Kakitani, A. Yoshimori and N. Mataga, *J. Phys. Chem.*, 1992, **96**, 5385–5392; (*c*) T. Kakitani, N. Matsuda, A. Yoshimori and N. Mataga, *Prog. React. Kinet.*, 1995, **20**, 347–375.
23 N. Nunthaboot, F. Tanaka, S. Kokpol, H. Chosrowjan, S. Taniguchi and N. Mataga, *J. Photochem. Photobiol., A*, 2009, **201**, 191–196.
24 N. Nunthaboot, F. Tanaka, S. Kokpol, H. Chosrowjan, S. Taniguchi and N. Mataga, *J. Phys. Chem. B*, 2008, **112**, 13121–13127.
25 N. Nunthaboot, F. Tanaka and S. Kokpol, *J. Photochem. Photobiol., A*, 2009, **207**, 274–281.
26 N. Nunthaboot, F. Tanaka and S. Kokpol, *J. Photochem. Photobiol., A*, 2010, **209**, 70–80.
27 H. Chosrowjan, S. Taniguchi, N. Mataga, T. Nakanishi, Y. Haruyama, S. Sato, M. Kitamura and F. Tanaka, *J. Phys. Chem. B*, 2010, **114**, 6175–6182.
28 K. Suto, K. Kawagoe, N. Shibata, K. Morimoto, Y. Higuchi, M. Kitamura, T. Nakaya and N. Yasuoka, *Acta Crystallogr., Sect. D: Biol. Crystallogr.*, 2000, **56**, 368–371.
29 D. Case, T. Darden, T. Cheatham, C. Simmerling, J. Wang, R. Duke, R. Luo, K. Merz, B. Wang, D. Pearlman, M. Crowley, S. Brozell, V. Tsui, H. Gohlke, J. Mongan, V. Hornak, G. Cui, P. Beroza, C. Schafmeister, J. Caldwell, W. Ross and P. Kollman, *AMBER, ver. 8*, University of California, San Francisco, 2004.
30 J. M. Wang, P. Cieplak and P. A. Kollman, *J. Comput. Chem.*, 2000, **21**, 1049–1074.
31 C. Schneider and J. Suhnel, *Biopolymers*, 1999, **50**, 287–302.
32 U. Essmann, L. Perera, M. L. Berkowitz, T. Darden, H. Lee and G. Pedersen, *J. Chem. Phys.*, 1995, **103**, 8577–8593.
33 J.-P. Ryckaert, G. Cicotti and H. J. C. Berendsen, *J. Comput. Phys.*, 1977, **23**, 327–341.
34 V. Vorsa, T. Kono, K. F. Willey and L. Winograd, *J. Phys. Chem. B*, 1999, **103**, 7889–7895.
35 E. R. Henry and R. M. Hochstrasser, *Proc. Natl. Acad. Sci. U. S. A.*, 1987, **84**, 6142–6146.
36 N. Nunthaboot, F. Tanaka, S. Kokpol, H. Chosrowjan, S. Taniguchi and N. Mataga, *J. Phys. Chem. B*, 2008, **112**, 15837–15843.
37 A. Yoshimori, T. Kakitani, Y. Enomoto and N. Mataga, *J. Phys. Chem.*, 1989, **93**, 8316–8323.
38 M. R. Gunner and P. L. Dutton, *J. Am. Chem. Soc.*, 1989, **111**, 3400–3412.
39 M. Iwaki, S. Kumazaki, K. Yoshihara, T. Erabi and S. Itoh, *J. Phys. Chem.*, 1996, **100**, 10802–10809.
40 C. Turro, J. M. Zaleski, Y. M. Karabatsos and D. G. Nocera, *J. Am. Chem. Soc.*, 1996, **118**, 6060–6067.
41 H. Yang, G. Luo, P. Karnchanaphanurach, T.-M. Louie, I. Rech, S. Cova, L. Xun and X. S. Xie, *Science*, 2003, **302**, 262–266.
42 G. Luo, I. Andricioaei, X. S. Xie and M. Karplus, *J. Phys. Chem. B*, 2006, **110**, 9363–9367.
43 H. Nishioka, N. Ueda and T. Kakitani1, *Biophysics*, 2008, **4**, 19–28.